Supporting information
Enhanced surface hydrophilicity improves osseointegration of titanium implants via integrin -mediated osteoimmunomodulation

Zheng Zheng [a], Shuaiqi Gan [a], Shuhan Yang [a], Chuping Hou [a], Zhimin Zhu [a], Hang Wang [a], Deping Yu [b], Zhiyong Qian [c], Hockin H. K. Xu [d-f], Wenchuan Chen [a *]

[a] State Key Laboratory of Oral Diseases & National Center for Stomatology & National Clinical Research Center for Oral Diseases & Department of Oral Prosthodontics, West China Hospital of Stomatology, Sichuan University, Chengdu 610041, Sichuan, China;
[b] School of Mechanical Engineering, Sichuan University, Chengdu 610041, China;
[c] State Key Laboratory of Biotherapy and Cancer Center, West China Hospital, Sichuan University, and Collaborative Innovation Center of Biotherapy, Chengdu 610041, Sichuan, China
[d] Biomaterials & Tissue Engineering Division, Department of Advanced Oral Sciences and Therapeutics, University of Maryland Dental School, Baltimore, MD 21201, USA;
[e] Center for Stem Cell Biology and Regenerative Medicine, University of Maryland School of Medicine, Baltimore, MD 21201, USA;
[f] University of Maryland Marlene and Stewart Greenebaum Cancer Center, University of Maryland School of Medicine, Baltimore, MD 21201, USA

For: *Journal of Materials Chemistry B*
(Submitted in October 2024)

* **Corresponding author:** Prof. Wenchuan Chen, email: hxkqcwc@scu.edu.cn.

Keywords: Surface hydrophilicity; Titanium; Integrin; Osteoimmunomodulation; Osseointegration; Surface functionalization

Materials and methods

NTAP treatment system

The novel NTAP treatment system for Ti activation was previously developed and described in our earlier work.[1,2] This system utilized a dielectric barrier discharge configuration with a quartz tube as the dielectric material between internal and external electrodes. The implant and collet both functioned as the coaxial internal electrode, while a copper tube covered the quartz tube, serving as the external electrode connected to the AC source's output. The system employed argon as the primary working gas to produce the NTAP on account of its cost-effectiveness and easy-to-ionize feature at a flow rate of 3000 sccm. Content 0.5% of oxygen was introduced to generate oxygen-containing groups. The working gases flowrates were accurately managed by two mass flow controllers (Laifeng, China).

Sample preparation

The commercial-grade polished pure Ti, and SLA disks (Xinhangfeng, China) were prepared in a cuboid with a length of 13.5 mm, a width of 6 mm, and a thickness of 1.9 mm. Cylindrical Ti implants were fabricated with SLA surfaces (2.0 mm in diameter, 3.5 mm in length, thread pitch 0.5 mm, WEGO, China). All Ti samples were split into four groups: (1) Control group for commercial-grade polished pure Ti (cTi), cTi untreated by NTAP; (2) Experimental group for cTi (N-cTi), disposed by NTAP for 30 s; (3) Control group for sand-blasted with large grit, acid-etched Ti (SLA), SLA untreated by NTAP; (4) Experimental group for SLA (N-SLA), subjected to 30 s

of NTAP treatment. NTAP-treated groups were instantaneously prepared before the following experiments to simulate clinical practice.

Surface characterizations

Ti samples' surface morphology was observed by FE-SEM (Inspect F50, FEI, USA). R_a values were measured through optical profilometer (Veeo Contour GT-K1, USA). Surface wettability was evaluated using a contact angle goniometer (OCA15EC, Dataphysics, Germany). Surface crystallinity was determined by an X-ray diffraction (XRD, Rigaku Ultima IV, Japan). Surface chemical states and elemental composition were assessed by XPS (Thermo Scientific K-Alpha+, USA). The C1s, Ti2p, N1s and O1s peaks were acquired, and all spectra's binding energy was calibrated with the C1s peak at 284.8 eV.

Protein Adsorption

Adsorption of FN (Solarbio, China) or FG (Sigma, USA) was conducted by immersing Ti samples in FN or FG solution with the concentration of 20 μg/mL at 37°C for 2 h. The total content of adsorbed FN and FG were quantified using a BCA protein assay kit (P0010, Beyotime, China) at 562-nm absorbance in a Varioskan LUX Multimode Microplate Reader (Thermo, USA). Adsorbed FN or FG activity and conformation were examined using ELISA at 450-nm absorbance and immunofluorescence staining in an inverted fluorescence microscope (Leica DMi8, Germany).

Cell culture

Two cell types, RAW264.7 mouse macrophage cell line (TIB-71, ATCC) and rat bone marrow mesenchymal stem cells (rBMMSCs), were applied in this study. RAW264.7 cells were cultured in Dulbecco's Modified Eagle Medium (DMEM, high glucose, Gibco, USA) supplemented with 10% fetal bovine serum (FBS, EVERY GREEN, BIOBASE, China) and 1% penicillin/streptomycin (PS, HyClone, USA) in a humidified incubator of 5% CO_2 at 37°C. At 80% confluence, adherent RAW264.7 cells were dislodged by flushing with culture medium and tapping the cell culture flask.

rBMMSCs were isolated from the bilateral femurs and tibias of 10-day-old male Sprague Dawley (SD) rats (West China Animal Experimental Center, Sichuan University). The cells were incubated with complete DMEM added with 15% FBS and 1% PS at 37°C with 5% CO_2. rBMMSCs were sub-cultured using trypsinization. The third and fourth passages of rBMMSCs was used for the following experiments at the density of 4.0×10^4 cells/ well on the Ti samples in 24-well plates in vitro. The identification of this rBMMSCs was through flow cytometry (CytoFLEX, Beckman Coulter, USA) by measuring the expression of CD29, CD90, CD11b, and CD45 (listed in Table S1).

Macrophage morphology, proliferation, and polarization *in vitro*

For cell morphology, proliferation assays, and immunofluorescence staining, RAW264.7 cells (4×10^4 cells/well) were seeded onto Ti samples in a 24-well plate. After overnight culture, lipopolysaccharide (LPS, 1 μg/ml, Sigma) was added to the complete DMEM for 2 h, and the medium was succeedingly removed and replaced with serum-free DMEM after 6 h.[3] The culture

medium of different groups was harvested and centrifuged (1200 rpm, 10 min) to acquire the supernatants for subsequent experiments. The secretion of cytokines (TNF-α, and IL-10) in these supernatants were quantitatively analyzed using a commercial mouse cytokine ELISA kit (SEA133Mu, SEA056Mu, Cloud Clone Corp, USA). RAW264.7 cells morphology adhered on the Ti surfaces was observed by FE-SEM. Cell counting kit-8 (CCK-8, Dojindo, Japan) assay was applied to evaluate cell proliferation on Ti disks after 1, 3 and 5 d of incubation by measuring the absorbance at 450 nm. Immunofluorescence staining was performed to analyze the expressions levels of CCR7 (M1 marker) and CD206 (M2 marker). All primary antibodies were presented in Table S1. iFluor™ 488 was used as secondary antibody. RAW264.7 cells also stained by TRITC Phalloidin and DAPI (Solarbio, China) to label the cellular actin filaments and cell nucleus, respectively. All stained RAW264.7 cells were observed in an inverted fluorescence microscope (Leica).

For purpose of further investigating the influence of NTAP on macrophage polarization, RAW264.7 cells (8×10^4 cells/well) were grown on different Ti surfaces in a 24-well plate. After 1 d of culture, the expression of CD86 (M1 marker, E-AB-F0994E, Elabscience, China) and CD206 (E-AB-F1135D, Elabscience) were identified using flow cytometry in CytoFLEX. At 1 and 4 d, RT-qPCR was implemented to quantify the expression levels of inflammatory cytokines, macrophage-phenotype markers, and autophagy-related, osteogenic-related, and osteoclastic-related molecules. Total RNA was isolated using a Trizol reagent (Thermo, USA), and cDNA was synthesized by a Hifair® II 1st Strand cDNA Synthesis Kit (11119ES60, YEASEN, China). RT-qPCR reactions were performed using the Hieff® qPCR SYBR Green Master Mix (11201ES08,

YEASEN) in QuantStudio^{TM} 7 Flex System (Applied Biosystems, Thermo, USA). Data were determined by the $2^{-\Delta\Delta CT}$ method and normalized to glyceraldehyde 3-phosphate dehydrogenase (*Gapdh*). All primer sequences used are presented in Table S2.

After 4 d of incubation, the protein expressions of macrophage-phenotype markers, and NF-κB signaling pathway were detected by Western blot. The primary and corresponding secondary antibodies were detailed in Table S1. Protein samples were estimated using an enhanced chemiluminescence kit (UE, China), and quantitatively analyzed by Image Lab software (3.0, Bio-Rad, USA).

RNA-Seq was applied to detect the macrophages gene expression profile on Ti surfaces. RAW 264.7 cells (1×10^5 cells/well) were seeded on Ti samples and cultured for 1 d after the stimulation of LPS and serum-free medium. Macrophages' RNA was extracted through a Trizol reagent. The whole-genome sequencing was performed by Sangon Biotech (China). Highly related genes and signaling pathway were analyzed using heatmaps, KEGG pathway analysis, and GO functional analysis.

Osteoimmunomodulation of Macrophages on rBMMSCs' biological behaviors *in vitro*

The culture medium for rBMMSCs (complete DMEM) was mixed with the collected supernatants of RAW264.7 cells at a ratio of 2:1 to prepare the MCM for following studies. After being cultured in MCM for 12 and 24 h, rBMMSCs' morphology was visualized by FE-SEM and a fluorescence microscope in TRITC Phalloidin and DAPI staining. rBMMSCs' proliferation on Ti disks after 1, 3 and 5 d of culture in MCM, was evaluated using CCK-8 assay.

After 24 h of incubation, the normal medium of was replaced with MCM supplemented with osteogenic components for subsequent osteogenic-related experiments. After 4, 7 and 14 d of osteogenic differentiation, ALP activity was performed using ALP Assay Kit (P0321, Beyotime, China) and BCA protein assay kit at 405 nm on a microplate reader. Alizarin red S (ARS) staining (1%, pH4.2, Solarbio, China) was conducted to evaluate the ECM calcification under a stereomicroscope (Olympus, Japan) at 14 and 21 d. Quantitative analysis of ARS staining was obtained with 10% cetylpyridinium chloride by calculating the absorbance at 562 nm. Following osteogenic induction for 4, 7 and 14 d in MCM, mRNA expressions of osteogenesis-related genes (*Alp*, *Runx2*, *Osx*, *Vegf*, *Opg*, *Ocn*, *Col1*, *Bmp-2*, and *Smad 1/3/4/5/8*, listed in Table S2) were assayed by RT-qPCR as rendered above. Protein expressions involved in osteogenesis (ALP, RUNX2, and OPG, details in Table S1) after 7 d of culture were determined through Western blot, as previously described.

The differential gene expression and function, highly correlated signaling pathway of rBMMSCs in MCM were identified by RNA-Seq. rBMMSCs were seeded at the density of 1.0×10^4 cells/disk, and underwent 7 d of osteogenic induction. The samples were collected and analyzed as aforementioned.

Integrin-mediated pathways *in vitro*

RAW264.7 cells were cultured as the abovementioned procedures. Immunofluorescence staining, RT-qPCR, and Western blot were used to analyze the expressions levels of integrin-

related adhesion proteins (Vinculin, and FAK), integrin β1 subfamily, and integrin β2 subfamily molecules.

siRNA (small interfering RNA) was used to inhibit integrins β1 and β2 expression, respectively. After RAW264.7 cells seeded on Ti samples at a density of 8×10^4 cells/well in serum-free medium overnight, the medium was replaced with the prepared transfected medium containing siRNA (50nM, Gene Pharma, China), EndoFectin™ Max (GeneCopoeia, USA), and serum-free DMEM. After 8 h of siRNA treatment, the transfected medium was substituted by complete DMEM. After 48 and 72 h of inhibition, relevant RT-qPCR and Western blot were accomplished to evaluate the expression levels of genes and proteins as described above, respectively. RAW264.7 cells were treated with Negative Control (NC) siRNA as controls.

PI3K inhibitor, LY294002 (L for short in Fig., S1737, Beyotime, China) was added to the cell medium at concentration of 20 μM for 1 d. The inhibitor concentration was determined on the grounds of manufacturer's recommendation and earlier published studies. After 3 d of culture, total RNA and proteins were harvested for the corresponding RT-qPCR and Western blot experiments.

In vivo animal model

All animal experiments were approved by State Key Laboratory of Oral Diseases & National Clinical Research Center for Oral Diseases (WCHSIRB-D-2021-003), and entire research protocols were executed conforming to the Animals in Research: Reporting *In Vivo* Experiments (ARRIVE) guidelines. Thirty male SD rats (4-week-old, mean weight: 90-110 g) were offered by West China Animal Experimental Center, Sichuan University. After 4 w of healing from the

extraction of bilateral maxillary first molars (M1), undersized holes were prepared for implants installation to gain the primary stability. The cylindrical Ti implants were randomized into NTAP-untreated and NTAP-treated groups. All the animals were injected with prophylactic antibiotic (80,000 units, Penicillin Potassium, Solarbio, China) daily for 3 d after surgery. After 2, 4 and 6 w of healing, animals were euthanized to harvest the maxillae containing implants.

Histological observation and immunostaining assay

All maxillae were fixed in 10% formalin for 24 h, and then decalcified with 10% ethylenediaminetetraacetic acid for following 30 d. Following removal of Ti implants, all samples were paraffin-embedded. Sections of 5 μm thickness were processed for the following staining. HE, Masson's trichrome, and TRAP staining were examined. The immunohistochemical staining of IL-10, CD86, and the CD206, as well as immunofluorescence staining of CD86, CD206, and DAPI were detected to evaluate the macrophages polarization around the implants. Stained sections were observed using an upright fluorescence microscope (Leica DM2000, Germany). The number of positive cells was calculated using ImageJ software (version 1.51v, USA).

Statistics analysis

All data were expressed as mean ± standard deviation (SD). Statistical differences and multiple comparisons among different groups were performed using one-way analysis of variance (ANOVA) or factorial analysis in IBM SPSS 22.0 statistical software (USA). A p value less than 0.05 was considered a statistically significant difference.

References

1 Z. Zheng, X. Ao, P. Xie, J. Wu, Y. Dong, D. Yu, J. Wang, Z. Zhu, H. Xu and W. Chen, *Sci Rep*, 2020, **10**, 10637.

2 Y. Dong, L. Long, P. Zhang, D. Yu, Y. Wen, Z. Zheng, J. Wu and W. Chen, *J Oral Sci*, 2021, **63**, 334-340.

3 L. Bai, P. Chen, Y. Zhao, R. Hang, X. Yao, B. Tang, C. Liu, Y. Xiao and R. Hang, *Biomaterials*, 2021, **278**, 121162.

Table S1. Detailed information about antibody

Antibody	Brand	Product code	Application proportion
Fibronectin	HUABIO	ET1702-25	ELISA and IF 1:250
Fibrinogen γ chain	HUABIO	ET7108-46	ELISA and IF 1:200
FITC anti-mouse/rat CD29	BioLegend	102205	FC 2 μL per 10^6 cells
FITC Anti-Rat CD90	Elabscience	E-AB-F1226C	FC 5 μL per test
FITC anti-rat CD11b	BioLegend	201805	FC 0.5 μL per 10^6 cells
FITC Anti-Rat CD45	Elabscience	E-AB-F1227C	FC 5 μL per test
CCR7	HUABIO	ET1602-22	WB 1:1000 IF 1:200
CD206	HUABIO	ET1702-04	WB 1:1000 IF 1:250
CD206	ProteinTech	60143-1-Ig	IHC/IF 1:300
Vinculin	HUABIO	ET1705-94	IF 1:200

FAK	HUABIO	ET1602-25	WB 1:1000 IF 1:100
Integrin β1 (ITGB1)	HUABIO	ET1601-17	WB 1:500
Integrin β2 (ITGB2)	HUABIO	ET1703-94	WB 1:1000
IκBα	HUABIO	ET1603-6	WB 1:2000
phospho-IκBα	HUABIO	ET1609-78	WB 1:1000
NF-κB p65	HUABIO	ET1603-12	WB 1:1000
phospho-NF-κB p65	ImmunoWay	YP0191	WB 1:1000
ALP	HUABIO	ET1601-21	WB 1:1000
RUNX2	Cell Signaling Technology	12556S	WB 1:1000
OPG	HUABIO	EM1701-98	WB 1:1000
PI3K	Cell Signaling Technology	4292S	WB 1:1000
phospho-PI3K	Cell Signaling Technology	4228S	WB 1:1000
AKT	Cell Signaling Technology	4691S	WB 1:1000
phospho-AKT	Cell Signaling Technology	4060S	WB 1:1000
GAPDH	Cell Signaling Technology	2118S	WB 1:1000
ACTB	ProteinTech	66009-1-Ig	WB 1:5000
CD86	Bioss	bs-1035R	IHC/IF 1:200
IL-10	Bioss	bs-0698R	IHC/IF 1:100
Goat anti-Mouse IgG Secondary Antibody HRP conjugated	SAB	L3032	WB 1:5000
Goat anti-Rabbit IgG Secondary Antibody HRP conjugated	SAB	L3012	ELISA 1:5000 WB 1:2000

iFluor™ 488 Conjugated Goat anti-rabbit IgG	HUABIO	HA1121	IF 1:800
Goat Anti-Mouse IgG H&L (Alexa Fluor 647)	ZENBIO	550047	IF 1:1000
Goat Anti-Rabbit IgG H&L (Alexa Fluor 488)	ZENBIO	550037	IF 1:1000
Note: FC: flow cytometry; WB: Western Blot; IHC: Immunohistochemistry; IF: Immunofluorescence			

Table S2. The primers sequences used for qRT-PCR

Gene	Forward primer sequence (5′-3′)	Reverse primer sequence (5′-3′)
	Mouse species	
Il6	ATAGTCCTTCCTACCCCAATTTCC	GATGAATTGGATGGTCTTGGTCC
Il18	TGGCCGACTTCACTGTACAAC	TGGGGTTCACTGGCACTTTG
Il1β	TGGAGAGTGTGGATCCCAAG	GGTGCTGATGTACCAGTTGG
Tnfα	CTGAACTTCGGGGTGATCGG	GGCTTGTCACTCGAATTTTGAGA
Cd86	CTGCTCATCATTGTATGTCAC	ACTGCCTTCACTCTGCATTTG
Cd11c	ACTTCACGGCCTCTCTTCC	CACCAGGGTCTTCAAGTCTG
Nos2	CACCAAGCTGAACTTGAGCG	CGTGGCTTTGGGCTCCTC
Cd206	AGACGAAATCCCTGCTACTG	CACCCATTCGAAGGCATTC
Cd163	CGTGTGCAGTGTCCAAAAGG	CACAAACCAAGAGTGCCGTG
Arg1	GGAATCTGCATGGGCAACCTGTGT	AGGGTCTACGTCTCGCAAGCCA
Il10	GAGAAGCATGGCCCAGAAATC	GAGAAATCGATGACAGCGCC

Lc3a	ACAGCATGGTGAGCGTCTC	AGGTTTCTTGGGAGGCGTAG
Lc3b	GATAATCAGACGGCGCTTGC	TCTCACTCTCGTACACTTCGG
Atg5	GATGCGGTTGAGGCTCAC	CTGTCATTCTGCAGTCCCATC
P62	AGCTGCTCTTCGGAAGTCAG	CTCCATCTGTTCCTCTGGCTG
Bmp2	GCTCCACAAACGAGAAAAGC	AGCAAGGGGAAAAGGACACT
Tgfβ1	CAGTACAGCAAGGTCCTTGC	ACGTAGTAGACGATGGGCAG
Vegfa	GTCCCATGAAGTGATCAAGTTC	TCTGCATGGTGATGTTGCTCTCTG
Trap	CACTCCCACCCTGAGATTTGT	CATCGTCTGCACGGTTCTG
Ctsk	GCAGCTCAACAAGGATACGG	GGTGCAGTTGGTCCAAGGTT
Integrin α5 (*Itga5*)	CTTCTCCGTGGAGTTTTACCG	GCTGTCAAATTGAATGGTGGTG
Integrin α2 (*Itga2*)	GGAACGGGACTTTCGCAT	GGTACTTCGGCTTTCTCATCA
Integrin β1 (*Itgb1*)	CCGCGCGGAAAAGATGAAT	CCACAATTTGGCCCTGCTTG
Integrin αM (*Itgam*)	CCATGACCTTCCAAGAGAATGC	ACCGGCTTGTGCTGTAGTC
Integrin αD (*Itgad*)	CATGAGATTCAGCCCTGTGGA	GTCACCTAGCTGGTCCAGTG
Integrin β2 (*Itgb2*)	CAGGAATGCACCAAGTACAAAGT	GTCACAGCGCAAGGAGTCA
Gapdh	TGACCACAGTCCATGCCATC	GACGGACACATTGGGGGTAG
	Rat species	
Alp	CGTCTCCATGGTGGATTATGCT	CCCAGGCACAGTGGTCAAG
Ocn	CATGAAGGCTTTGTCAGACT	CTCTCTCTGCTCACTCTGCT
Col1	GGTCCCAAAGGTGCTGATGG	GACCAGGCTCACCACGGTCT
Runx2	GAACCAAGAAGGCACAGAC	AATGCGCCCTAAATCACTG

Osx	CGGCAAGGCTTCGCATCTG	GGAGCAGAGCAGACAGGTGAACT
Opg	TCAAGAATGCCACAGAA	GTCACGAAGCGGGTGTAGT
Bmp-2	GAAGCCAGGTGTCTCCAAGAG	GTGGATGTCCTTTACCGTCGT
Vegf	GGCTCTGAAACCATGAACTTTCT	GCAGTAGCTGCGCTGGTAGAC
Smad1	AAGCCTCTGGAATGCTGCGA	GCTGATTTGTCCCAGGTTTCG
Smad3	ACAAGGTCCTCACCCAGATG	TGGCGATACACCACCTGTTA
Smad4	GGCTGGTCGGAAAGGATT	GTGGGTAAGGATGGCTGT
Smad5	GCCTATGGACACAAGCAACA	AGGCAACAGGCTGAACATCT
Smad8	ACCATTACCGCAGAGTGGAG	TGAGGGTTGTACTCGCTGTG
Gapdh	ACAGCAACAGGGTGGTGGAC	TTTGAGGGTGCAGCGAACTT

Table S3. Atomic percentage (at %) of all elements and C/O ratio

Group	O1s (at %)	Ti2p (at %)	C1s (at %)	N1s (at %)	C/O Ratio
cTi	34.25	12.45	51.35	1.94	1.50
N- cTi	54.78	18.8	23.59	2.82	0.43
SLA	36.43	11.64	50.24	1.7	1.40
N-SLA	53.6	22.74	22.26	1.39	0.42

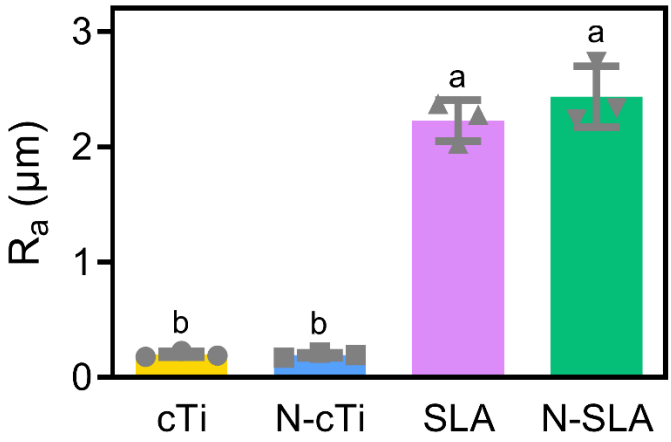

Fig. S1. Surface roughness of R_a values. Results are shown with mean ± SD; n = 3 independent samples per group. Values with dissimilar letters are significantly different ($p < 0.05$).

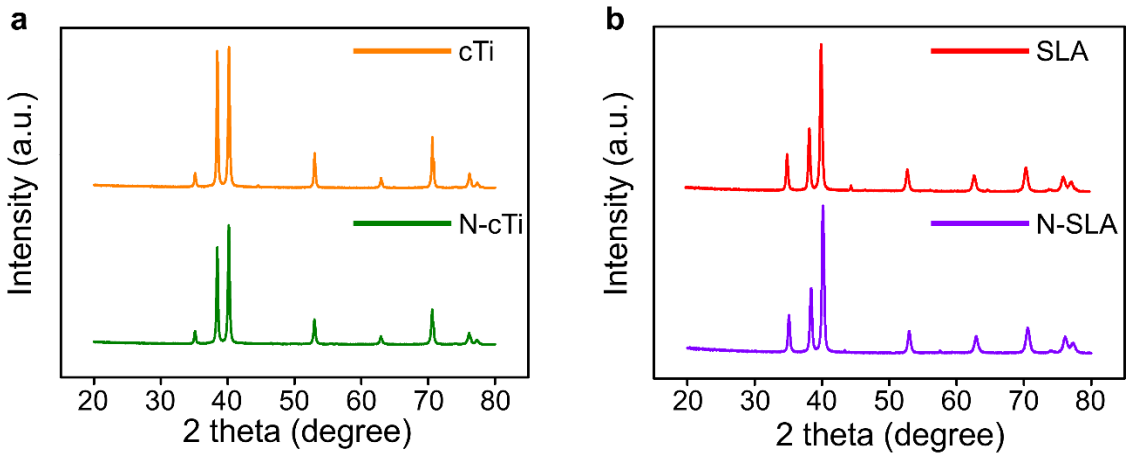

Fig. S2. XRD spectrum of cTi, N-cTi (a), SLA, and N-SLA (b).

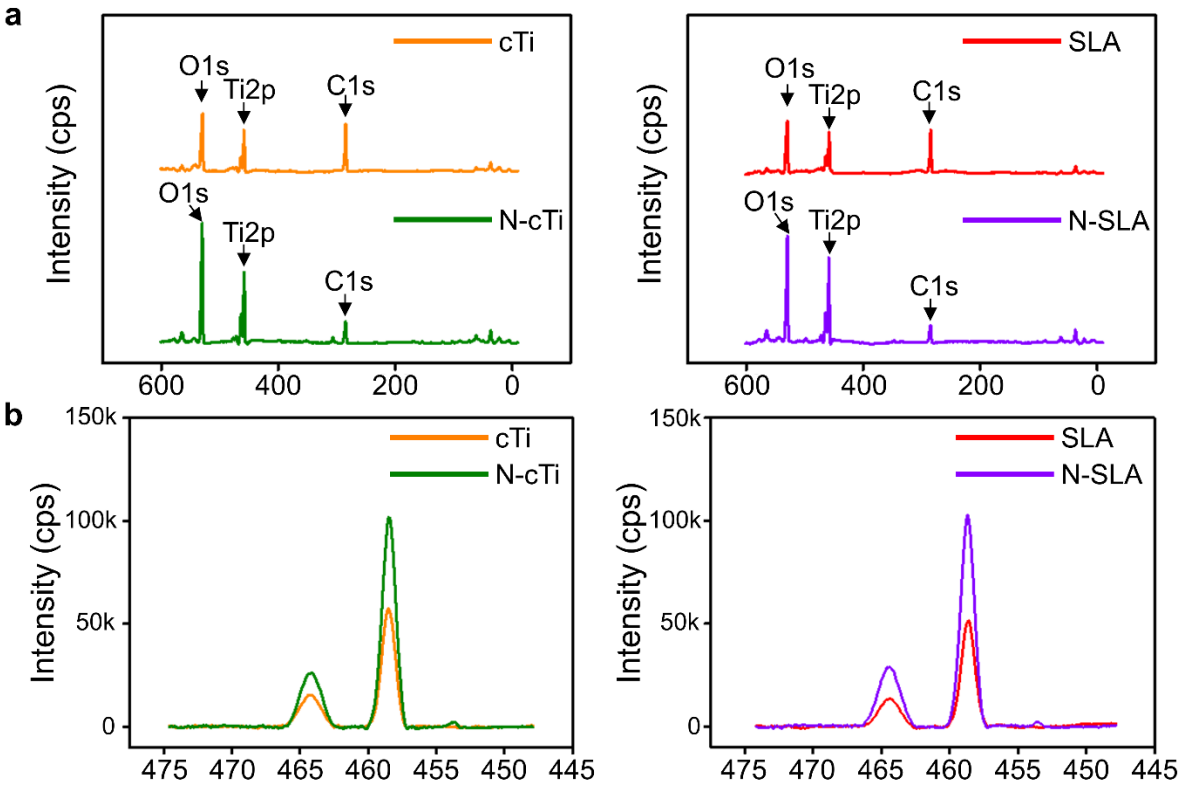

Fig. S3. (a) XPS spectra of cTi, N-cTi, SLA, and N-SLA showed O1s, Ti2p and C1s peaks. (b) High resolution spectra of Ti2p.

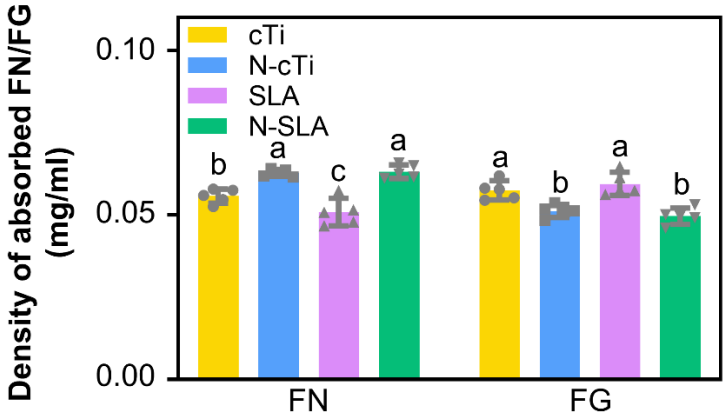

Fig. S4. Amount of FN and FG adsorption measured by BCA (n = 6 independent samples per group). Results are shown with mean ± SD. Values with dissimilar letters are significantly different ($p < 0.05$).

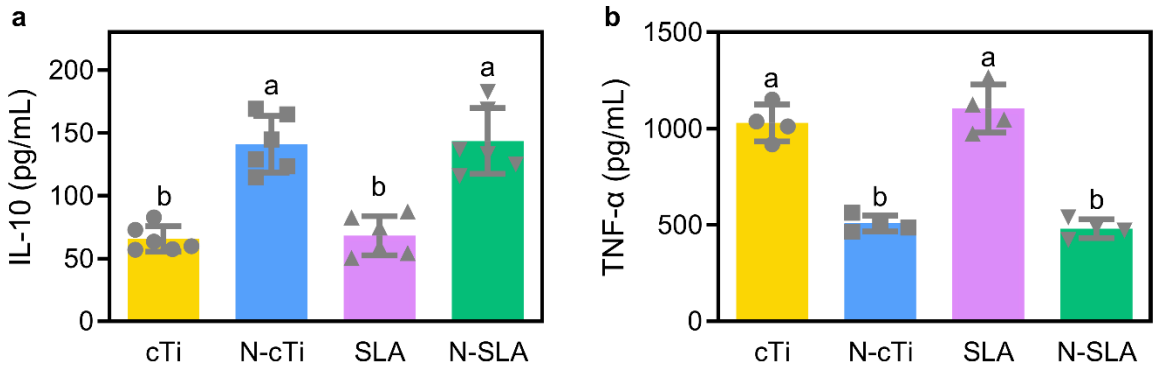

Fig. S5. (a) TNF-α and (b) IL-10 cytokine secretion by ELISA.

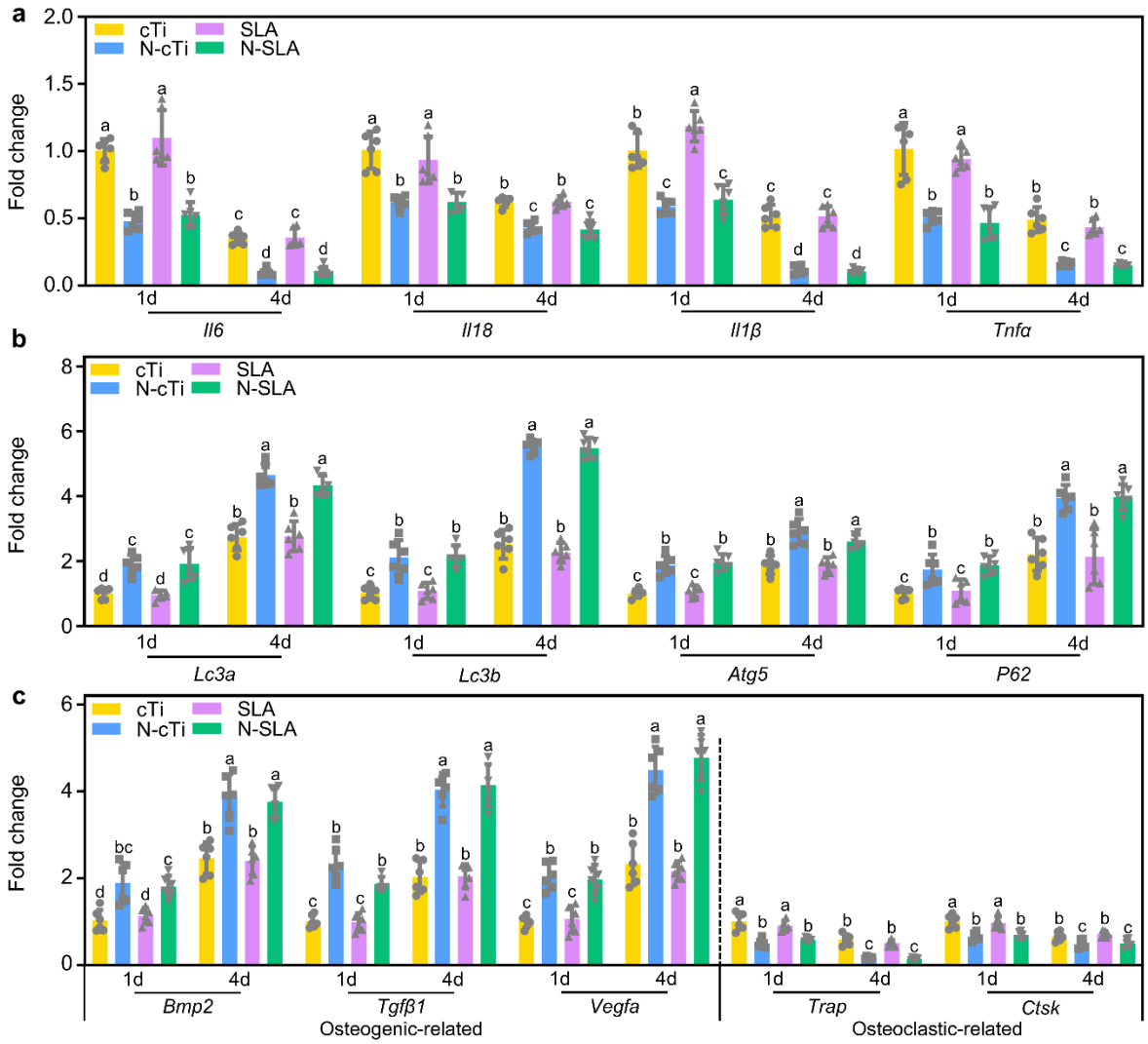

Fig. S6. (a-c) qRT-PCR results of inflammatory cytokines (*Il6*, *Il18*, *Il1β*, and *Tnfα*), autophagy-related molecules (*Lc3a*, *Lc3b*, *Atg5*, and *P62*), osteogenic-related molecules (*Bmp2*, *Tfgβ1*, and

Vegfa), and osteoclastic-related molecules (*Trap*, and *Ctsk*). Results are shown with mean ± SD; n = 6 independent samples per group. Values with dissimilar letters are significantly different ($p < 0.05$).

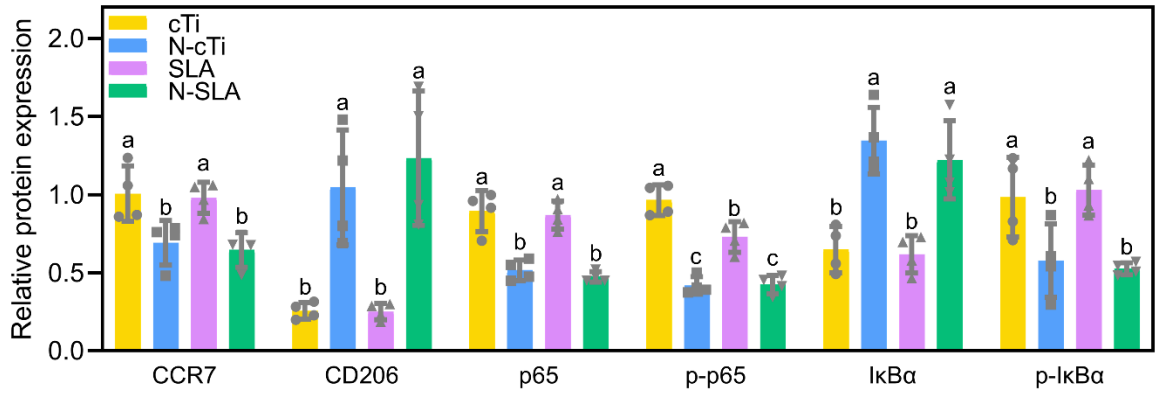

Fig. S7. Western blot's semi-quantification of CCR7, CD206, p65, IκBα, and phosphorylation of p65 and IκBα compared to GAPDH expression (n = 4 independent samples per group).

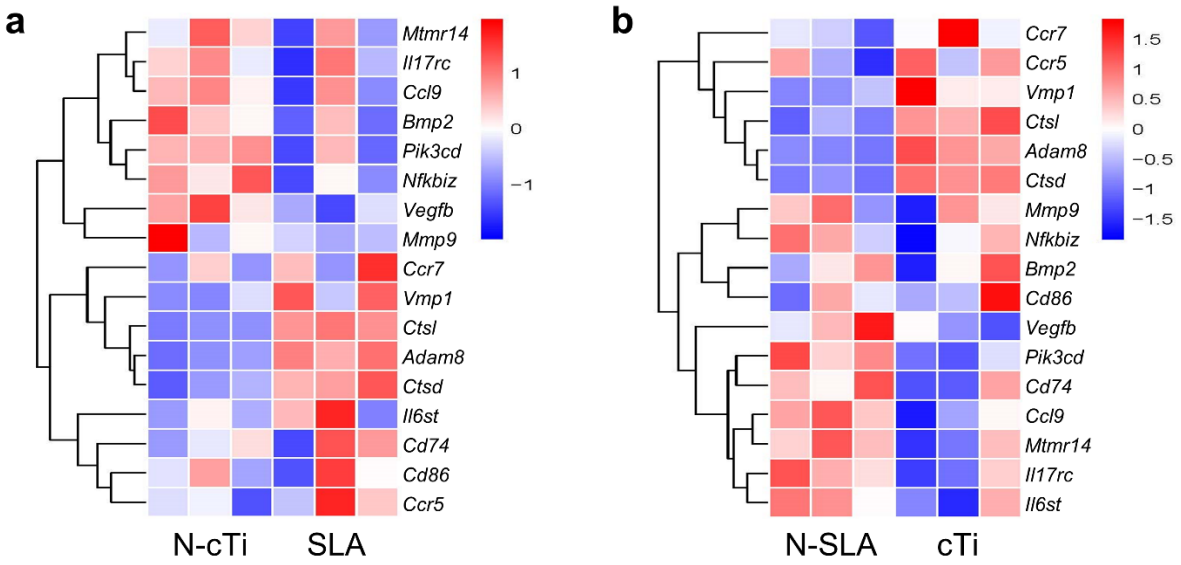

Fig. S8. RNA-Seq analysis of macrophages on different surfaces. (a, b) Heatmaps of distinct upregulated and downregulated genes of N-cTi vs SLA, and N-SLA vs cTi, respectively.

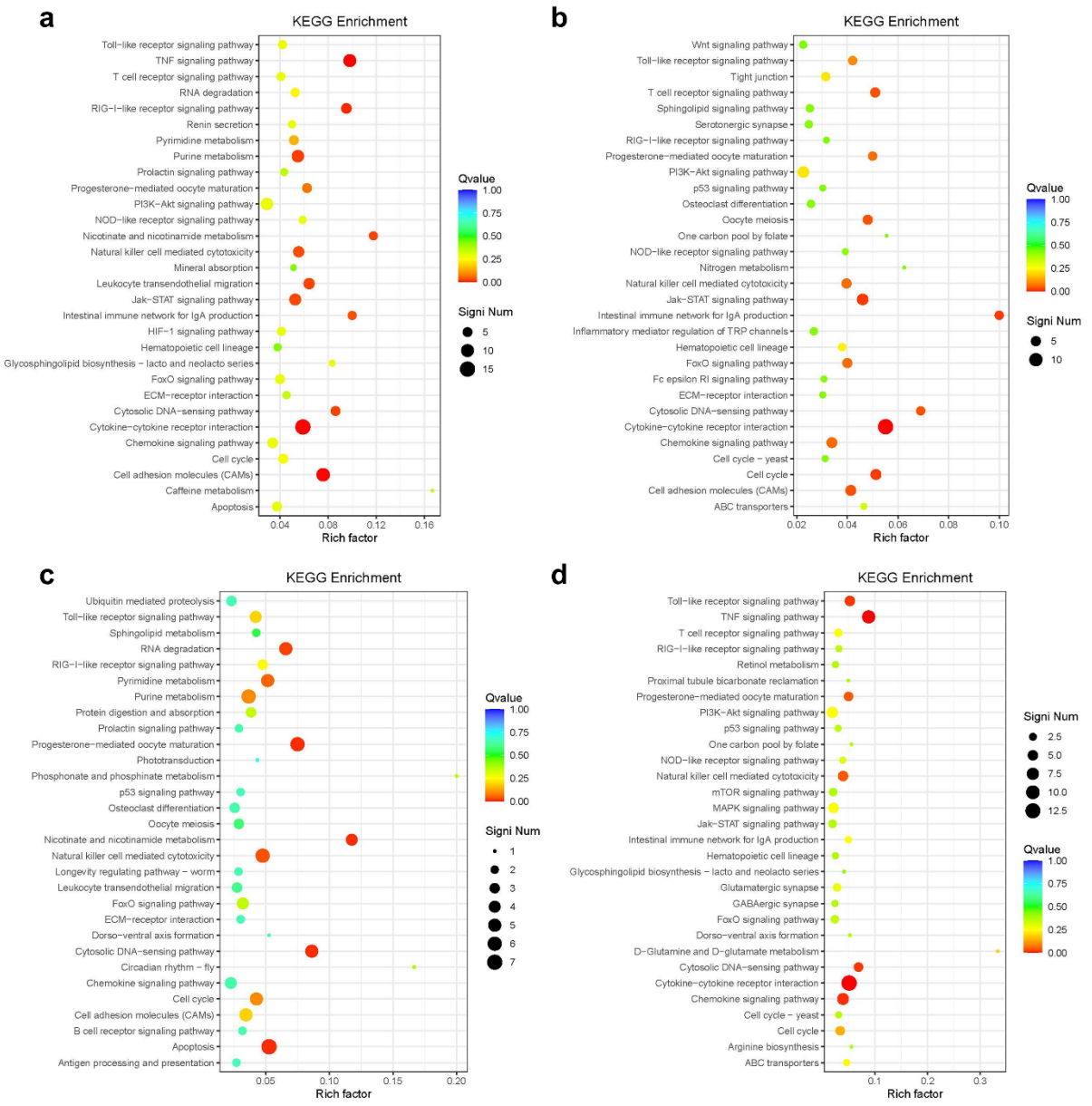

Fig. S9. RNA-Seq analysis of macrophages on different surfaces. (a-d) Upregulated pathways analyzed by KEGG pathway method of N-cTi vs cTi, N-cTi vs SLA, N-SLA vs cTi, and N-SLA vs SLA, respectively. n = 3 independent samples per group.

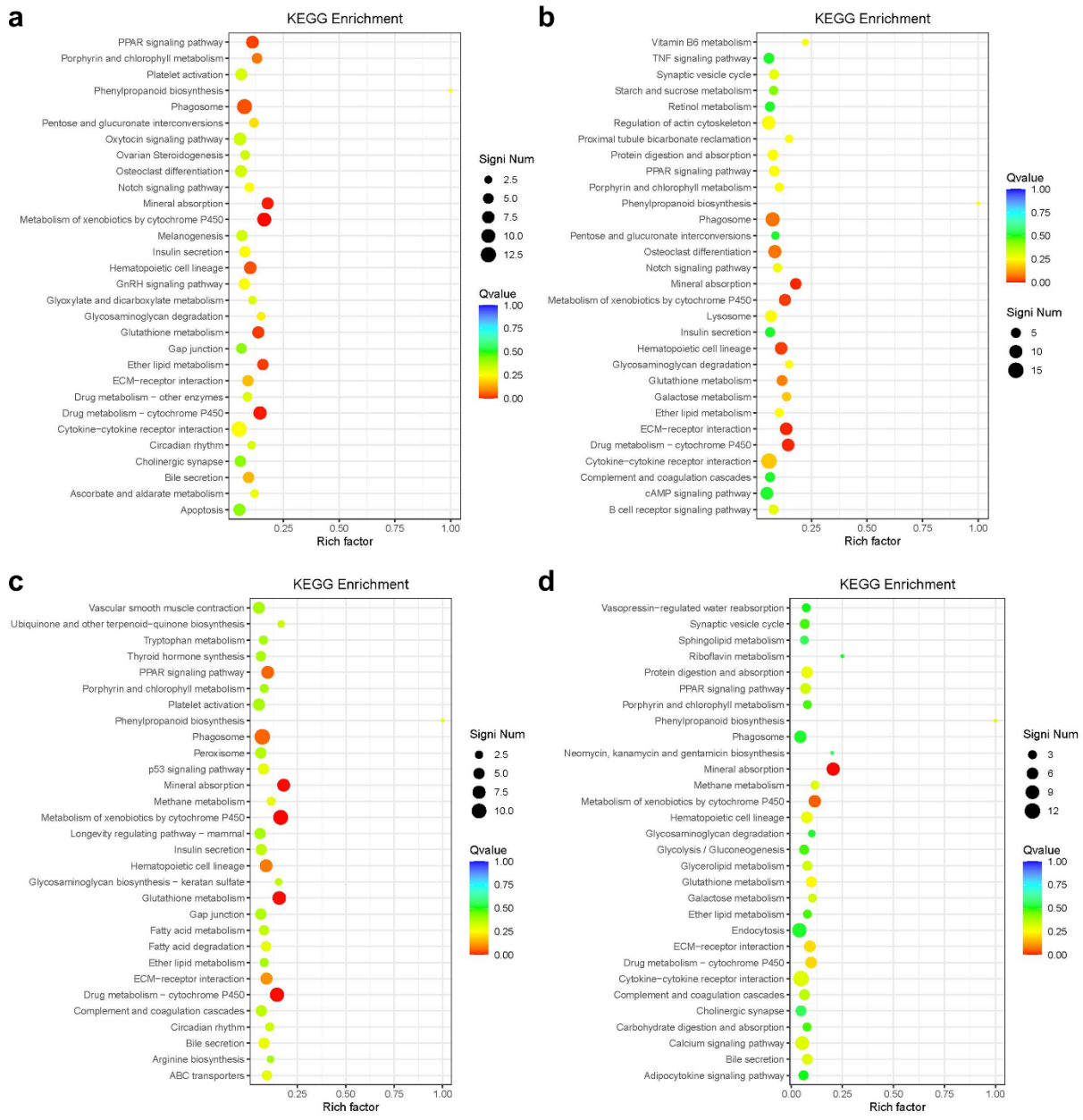

Fig. S10. RNA-Seq analysis of macrophages on different surfaces. (a-d) Downregulated pathways analyzed by KEGG pathway method of N-cTi vs cTi, N-cTi vs SLA, N-SLA vs cTi, and N-SLA vs SLA, respectively. n = 3 independent samples per group.

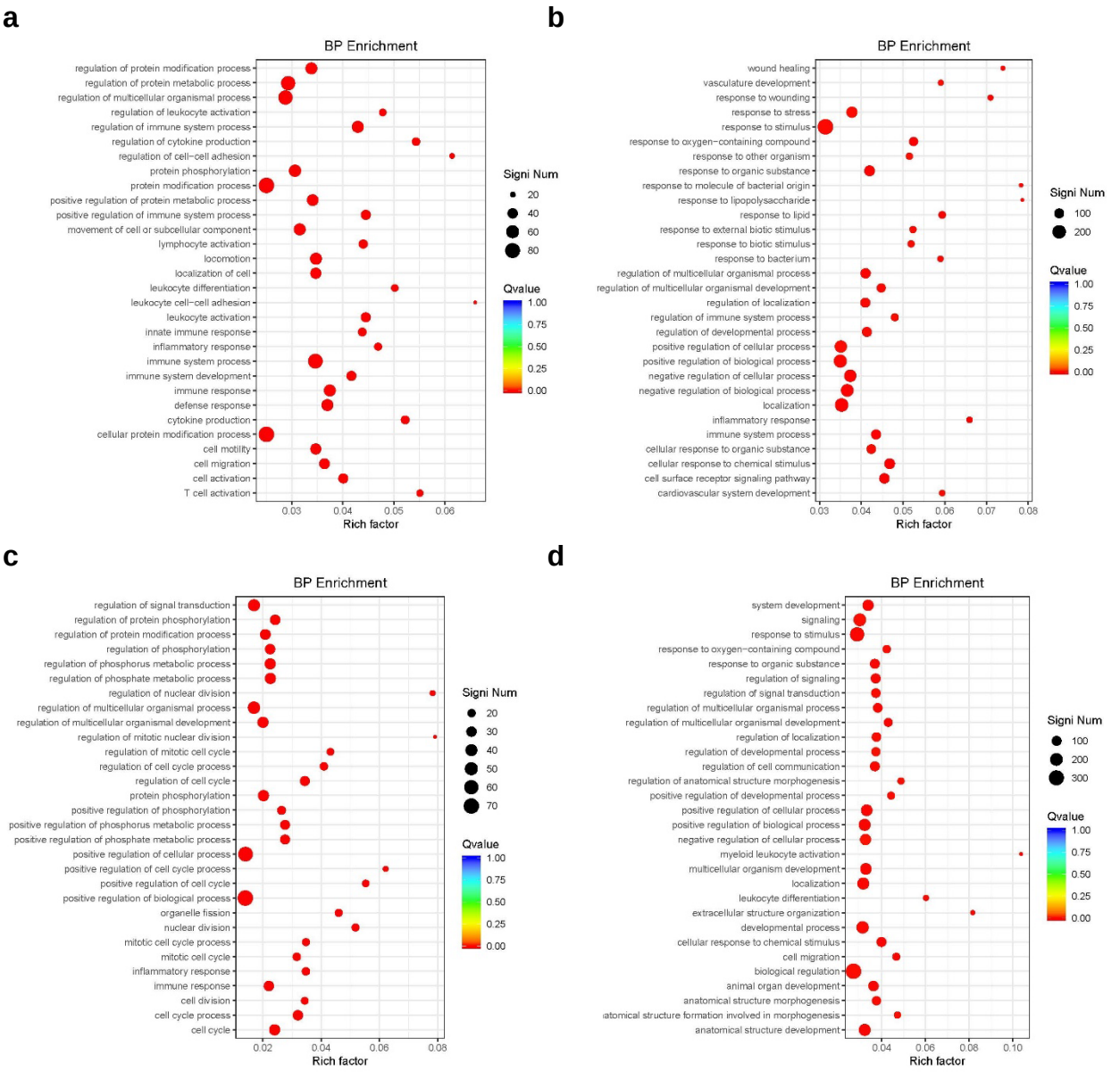

Fig. S11. RNA-Seq analysis of macrophages on different surfaces. (a, c) Upregulated biological process by GO enrichment analysis of N-cTi vs cTi, and N-SLA vs SLA, respectively. (b, d) Downregulated biological process of N-cTi vs cTi, and N-SLA vs SLA, respectively. n = 3 independent samples per group.

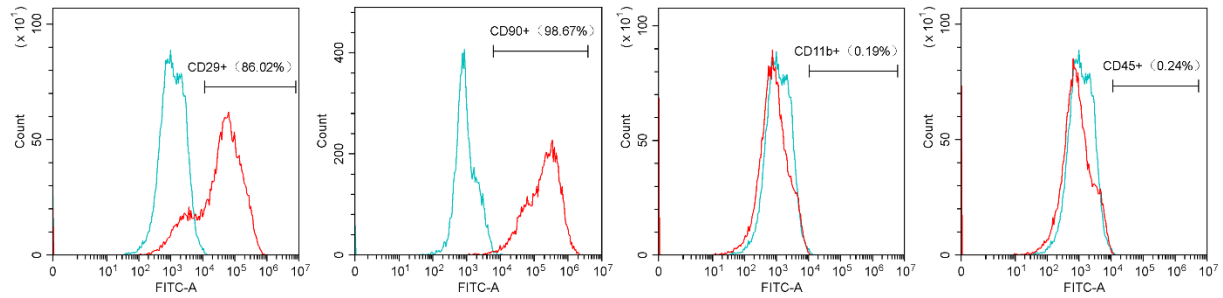

Fig. S12. rBMMSCs' surface markers confirmed by flow cytometry.

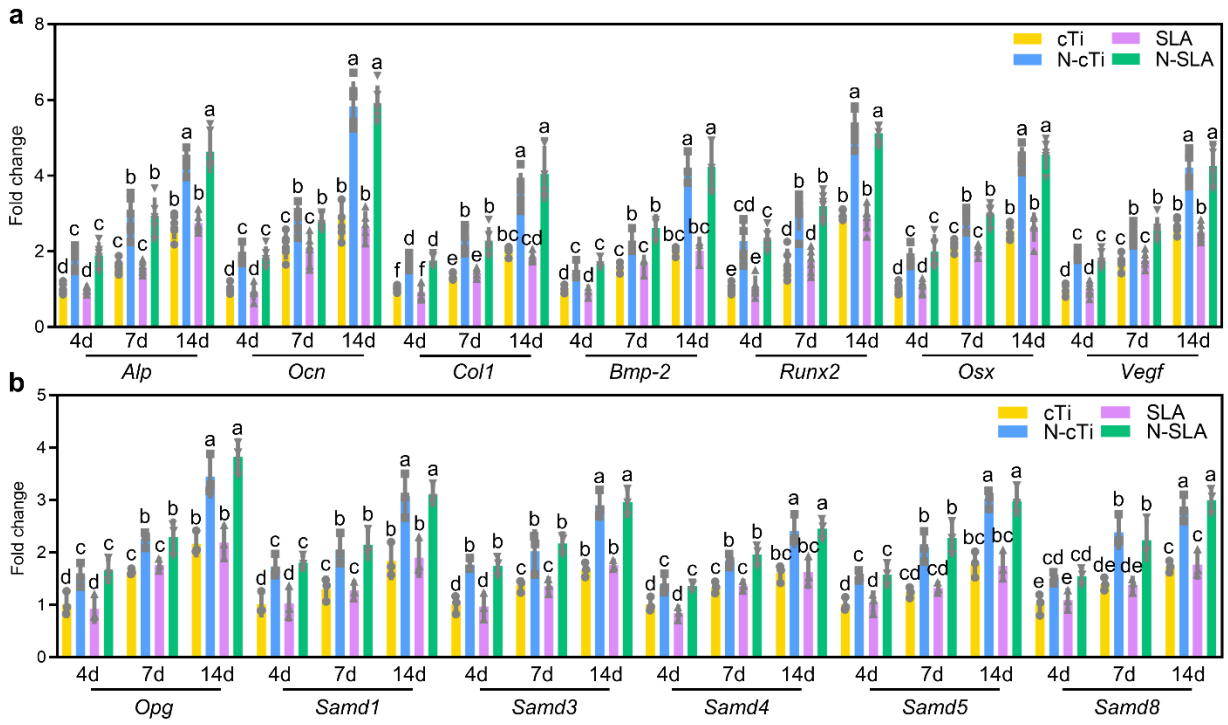

Fig. S13. (a) The mRNA expressions of osteogenesis-related genes (*Alp*, *Ocn*, *Col1*, *Bmp-2*, *Runx2*, *Osx*, and *Vegf*) of rBMMSCs cultured in MCM detected using qRT-PCR (n = 6 independent samples per group). (b) The mRNA expressions of osteogenesis-related genes (*Opg*) and SMADs (*Smad1*, *3*, *4*, *5*, and *8*) of the rBMMSCs cultured in MCM, n = 6 independent samples per group. Results are shown with mean ± SD. Values with dissimilar letters are significantly different ($p < 0.05$).

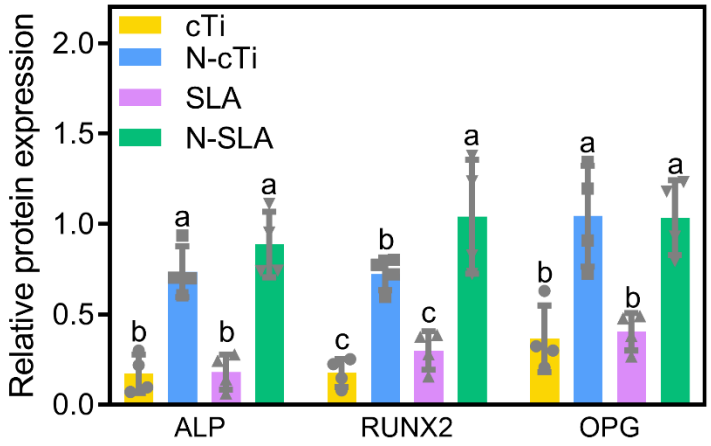

Fig. S14. Western blot's semi-quantification of ALP, RUNX2, and OPG compared to ACTB expression, n = 4 independent samples per group. Results are shown with mean ± SD. Values with dissimilar letters are significantly different ($p < 0.05$).

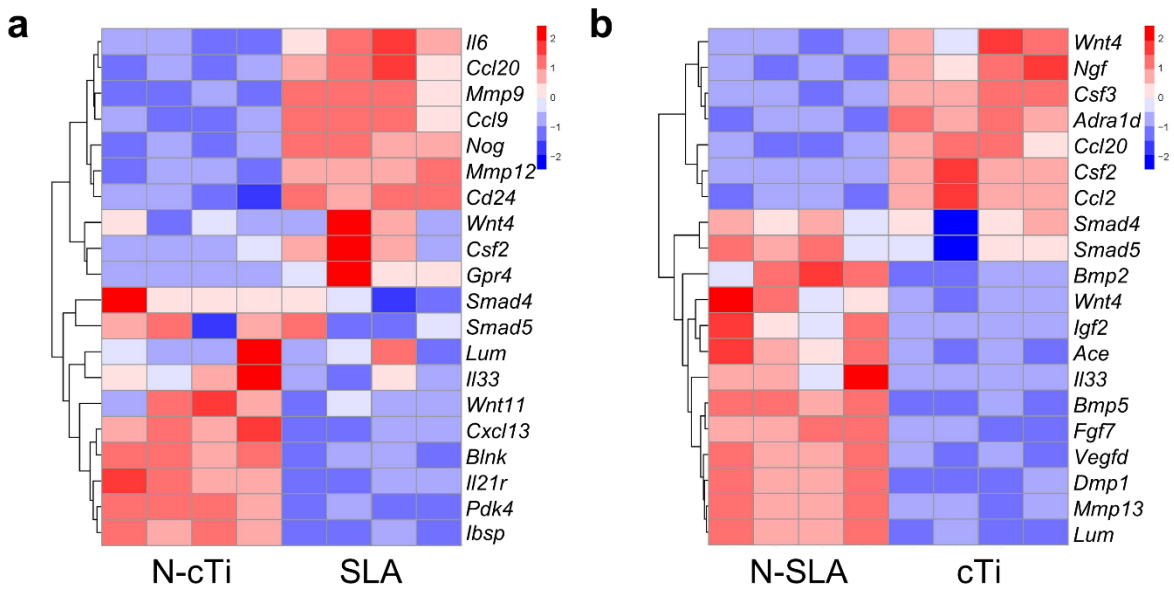

Fig. S15. RNA-Seq analysis of rBMMSCs after osteogenic induction for 7 d in MCM. (a, b) Heatmaps of distinct upregulated and downregulated genes of rBMMSCs in N-cTi vs SLA, and N-SLA vs cTi, respectively.

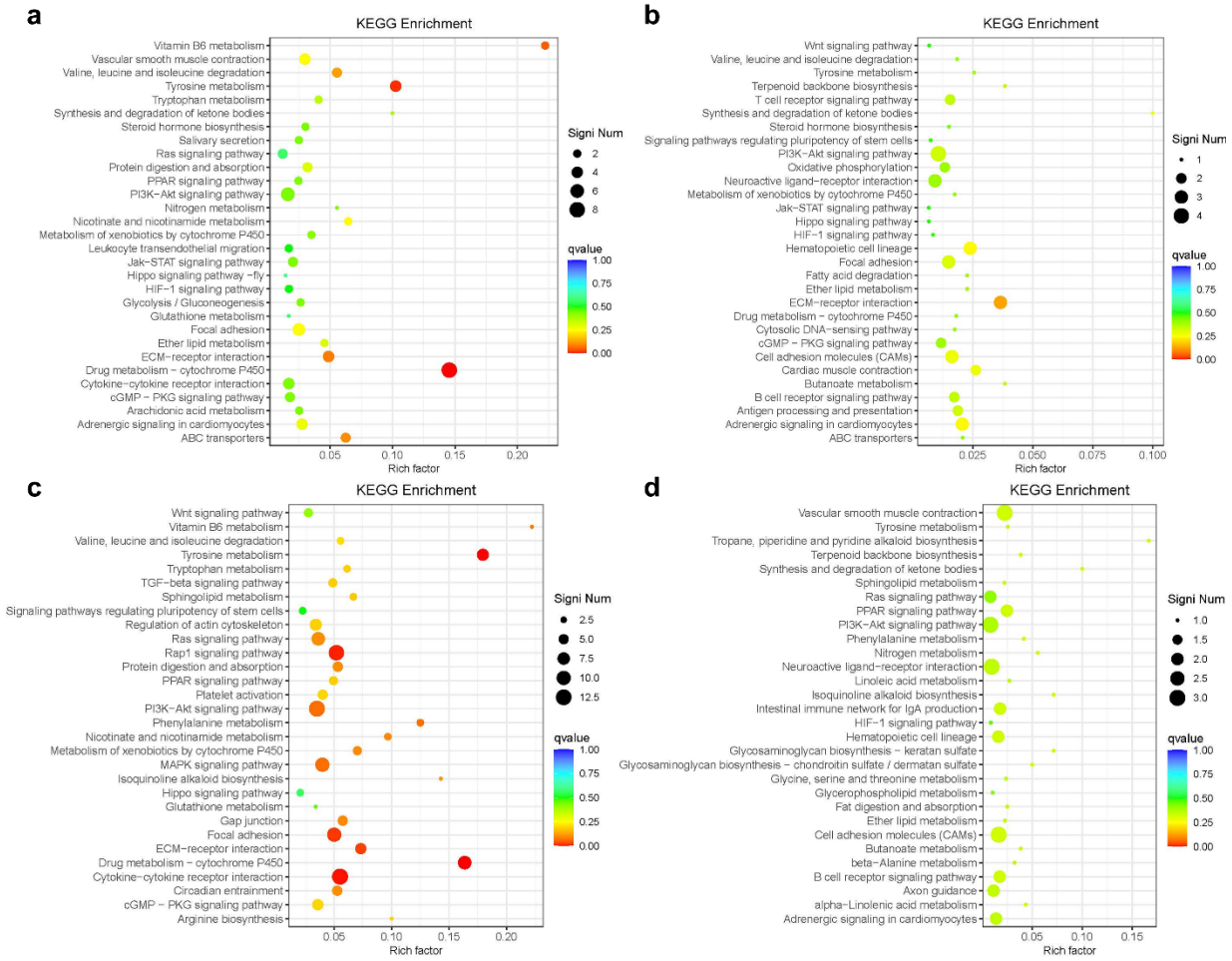

Fig. S16. RNA-Seq analysis of rBMMSCs after osteogenic induction for 7 d in MCM. (a-d) Upregulated pathways analyzed by KEGG pathway method of N-cTi vs cTi, N-cTi vs SLA, N-SLA vs cTi, and N-SLA vs SLA, respectively. n = 4 independent samples per group.

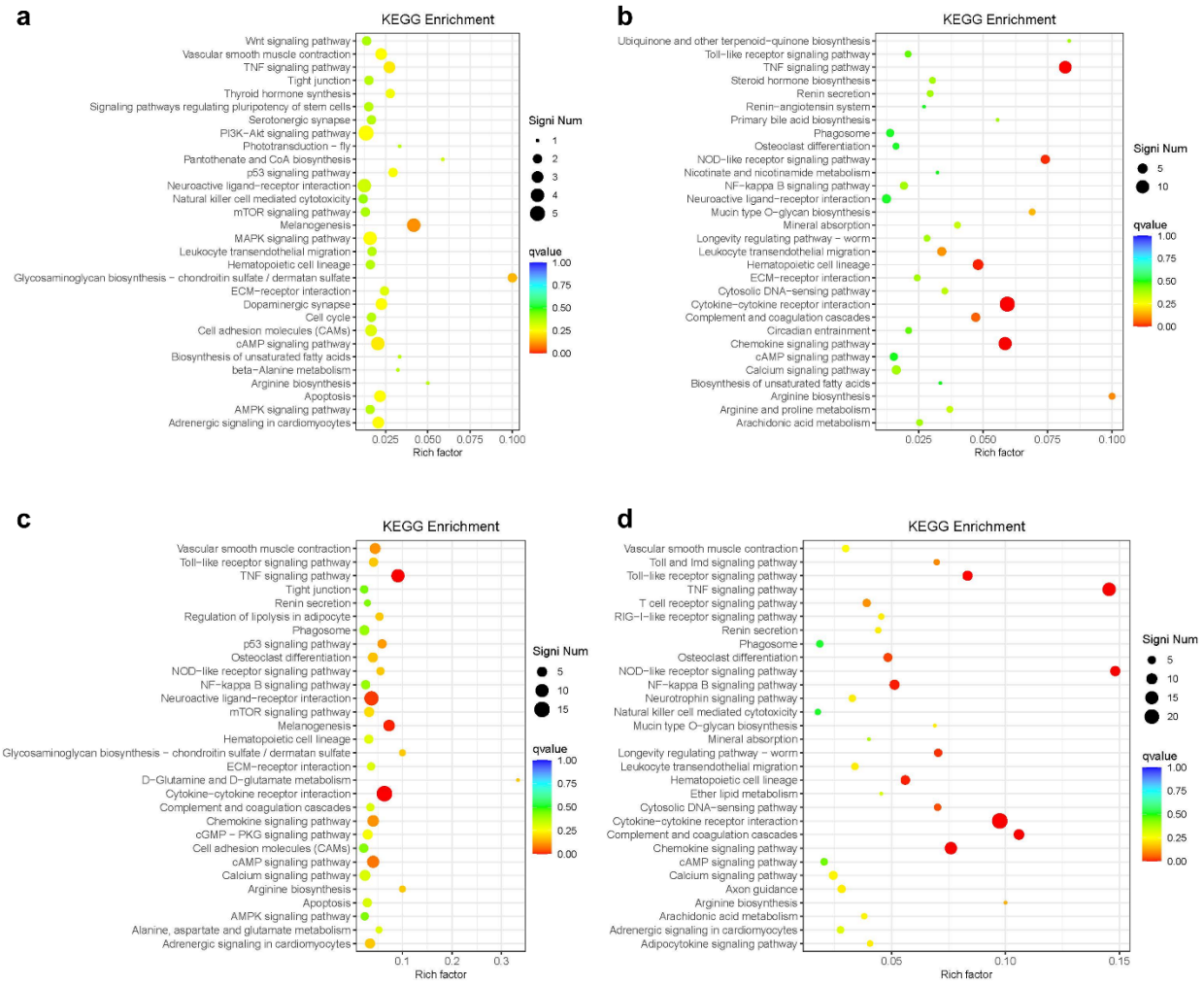

Fig. S17. RNA-Seq analysis of rBMMSCs after osteogenic induction for 7 d in MCM. (a-d) Downregulated pathways of N-cTi vs cTi, N-cTi vs SLA, N-SLA vs cTi, and N-SLA vs SLA, respectively. n = 4 independent samples per group.

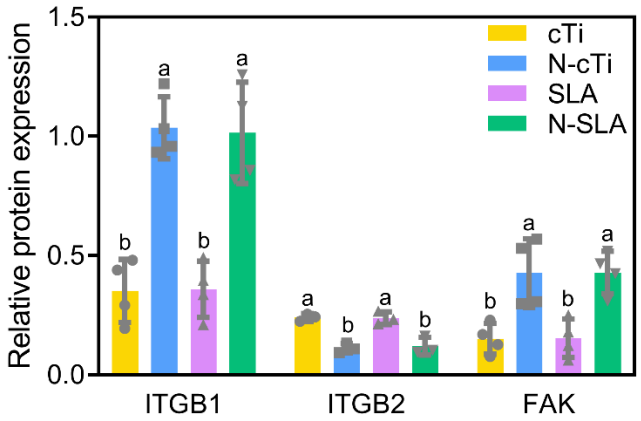

Fig. S18. Western blot's semi-quantification of ITGB1, ITGB2, and FAK compared to GAPDH expression (n = 4 independent samples per group).

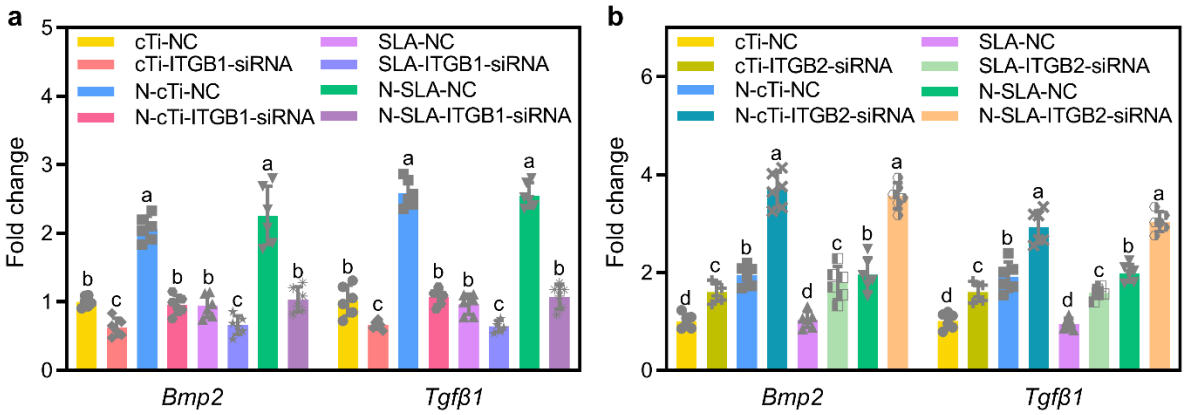

Fig. S19. (a, b) Effects of ITGB1 and ITGB2 knockdown on gene expressions of *Bmp2* and *Tgfβ1*. Results are shown with mean ± SD; n = 6 independent samples per group. Values with dissimilar letters are significantly different ($p < 0.05$).

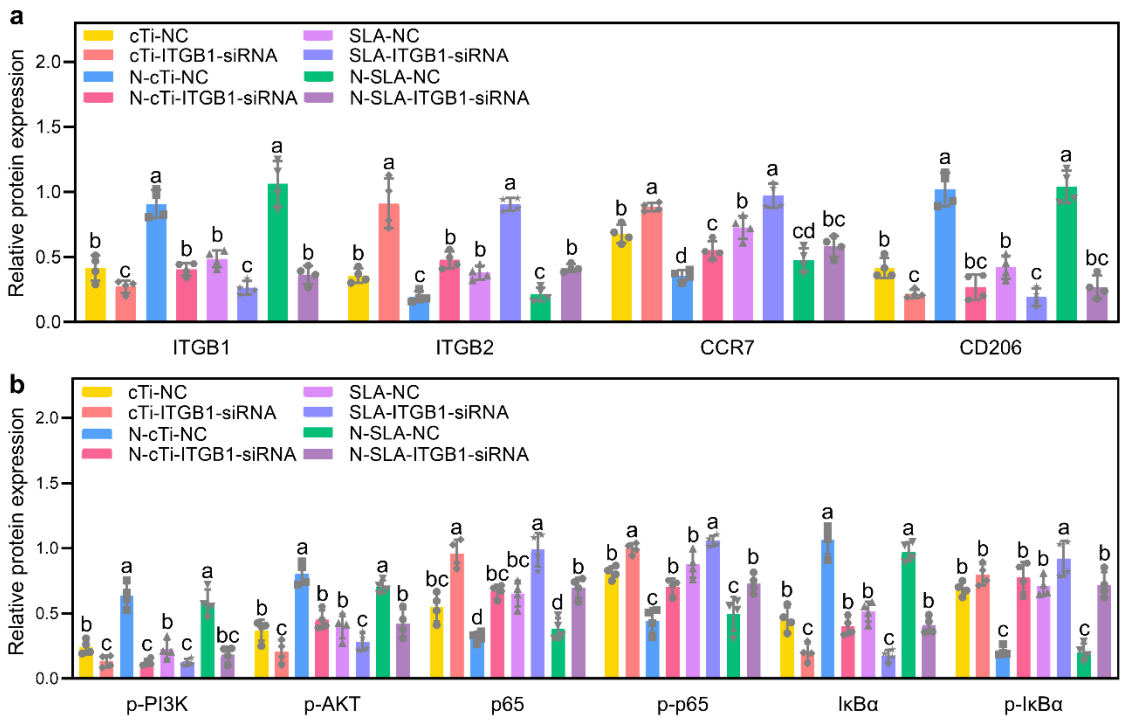

Fig. S20. (a, b) Western blot's semi-quantification of integrin subfamily, macrophage polarization markers, PI3K/Akt, and NF-κB signaling pathways in ITGB1-inhibited cells (n = 4 independent samples per group). Results are shown with mean ± SD. Values with dissimilar letters are significantly different ($p < 0.05$).

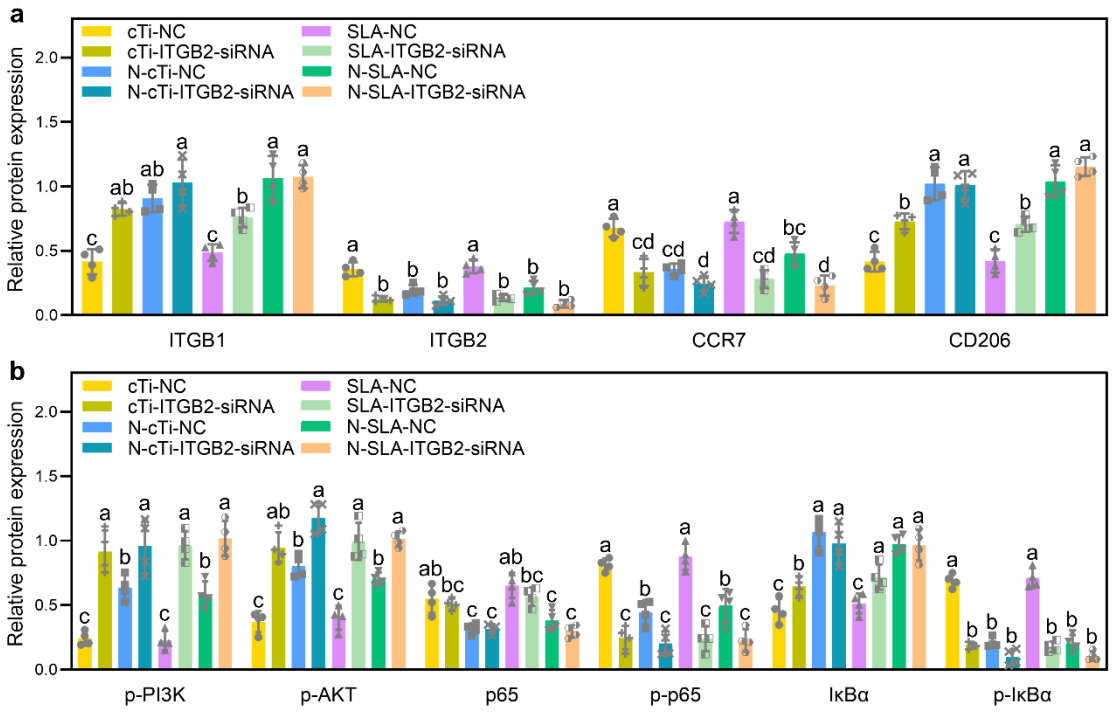

Fig. S21. (a, b) Western blot's semi-quantification of integrin subfamily, macrophage polarization markers, PI3K/Akt, and NF-κB signaling pathways in ITGB2-inhibited cells (n = 4 independent samples per group). Results are shown with mean ± SD. Values with dissimilar letters are significantly different ($p < 0.05$).

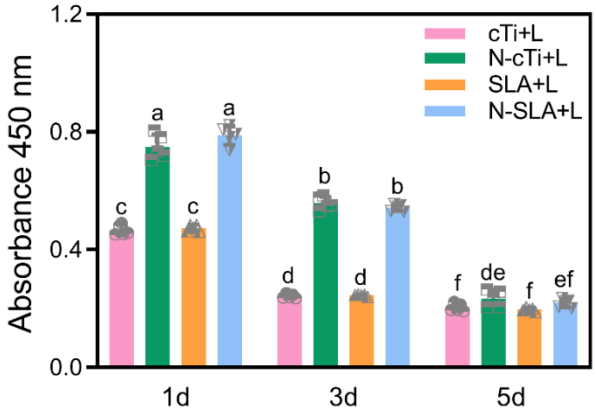

Fig. S22. Cell proliferation of RAW264.7 cells in the presence of PI3K inhibitor (LY294002) after 1, 3 and 5 d of culture. Results are shown with mean ± SD; n = 6 independent samples per group. Values with dissimilar letters are significantly different ($p < 0.05$).

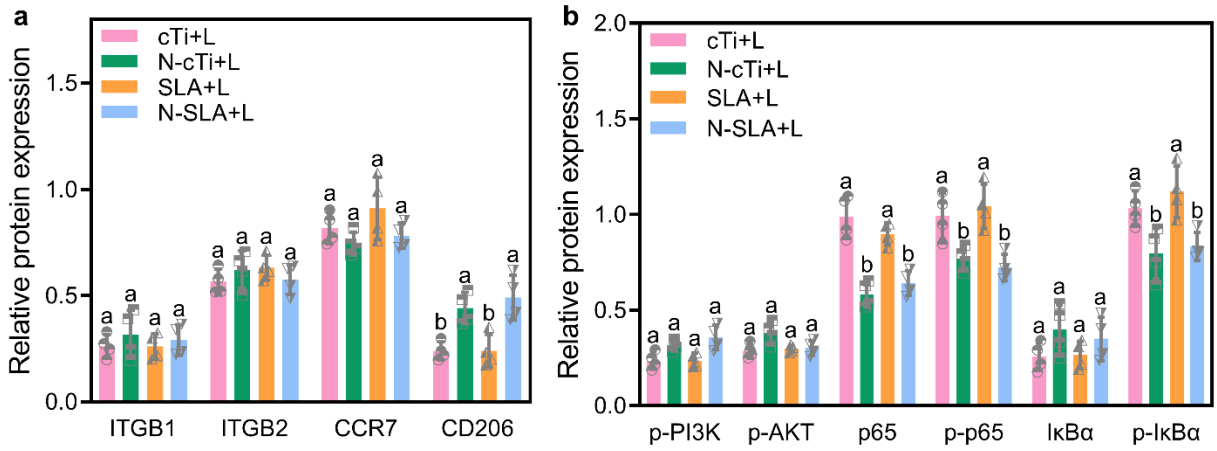

Fig. S23. (a, b) Western blot's semi-quantification of integrin subfamily, macrophage polarization markers, PI3K/Akt, and NF-κB signaling pathways in the presence of PI3K inhibitor (n = 4 independent samples per group). Results are shown with mean ± SD. Values with dissimilar letters are significantly different ($p < 0.05$).

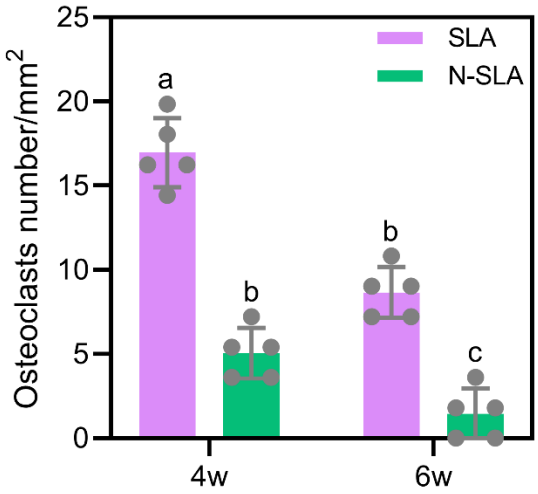

Fig. S24. Osteoclast number's quantitative results (n = 5 independent samples per group). Results are shown with mean ± SD. Values with dissimilar letters are significantly different ($p < 0.05$).

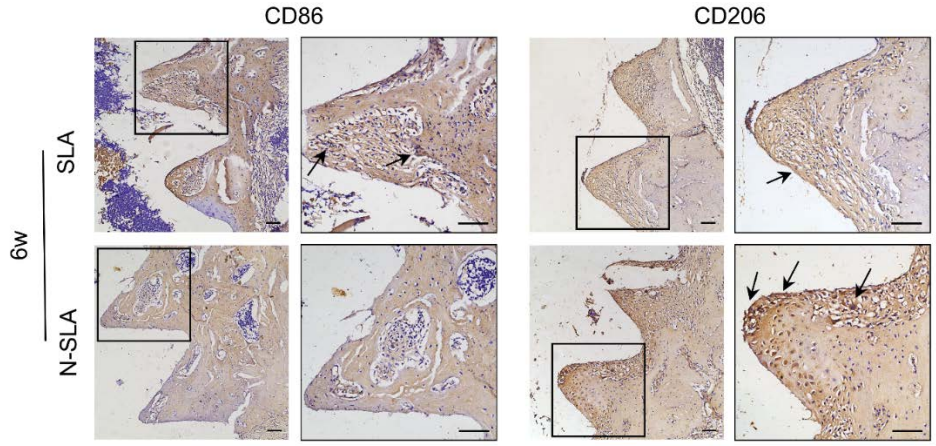

Fig. S25. Immunohistochemical staining of CD86 (M1 marker) and CD206 (M2 marker) around implant at 6 w. Arrow heads denoted CD86- or CD206-positive cells. Scar bar = 100 μm.

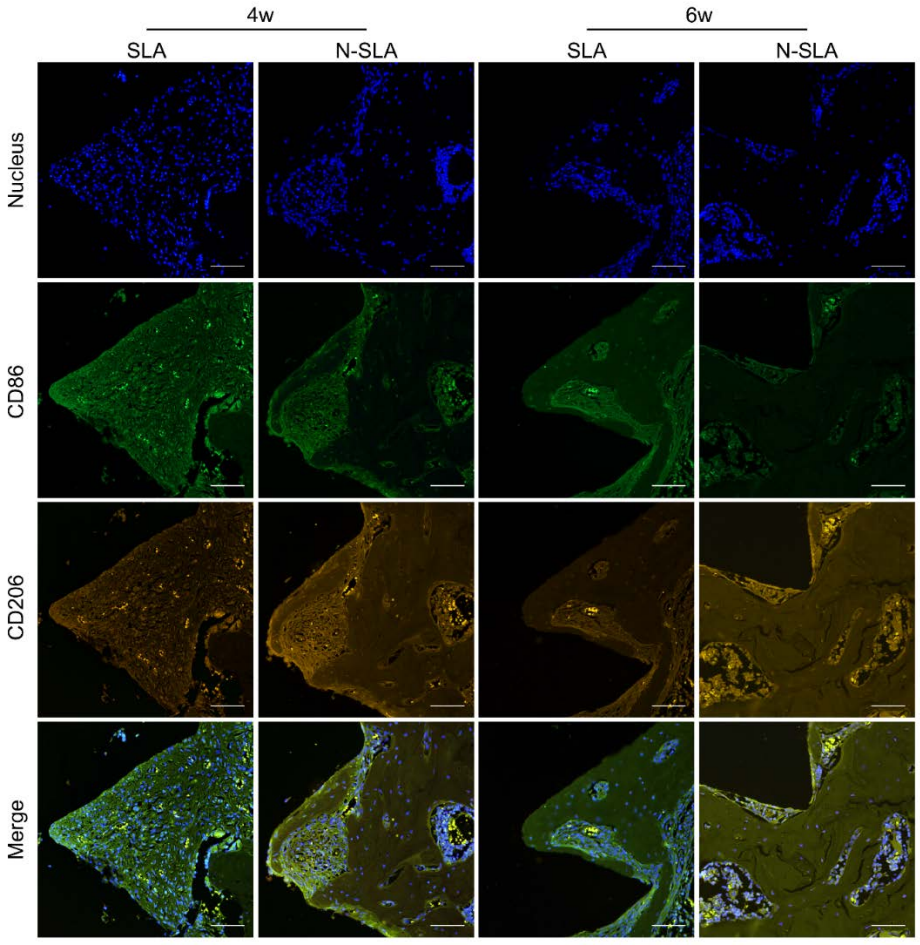

Fig. S26. Immunofluorescent staining of CD86 (green), CD206 (red) and nuclei (blue) in peri-implant tissue. Scar bar = 100 μm.